Crystal Growth Hot Paper

International Edition: DOI: 10.1002/anie.201603687
German Edition: DOI: 10.1002/ange.201603687

Determination of the Preassembled Nucleating Units That Are Critical for the Crystal Growth of the Metal–Organic Framework CdIF-4

*Raghidah Wagia, Ilya Strashnov, Michael W. Anderson, and Martin P. Attfield**

Abstract: *Identifying the form and role of the chemical species that traverse the stages of crystallization is critical to understanding the formation process of coordination polymers. Herein, we report the combined use of in situ atomic force microscopy and mass spectrometry to identify preformed, complex, cadmium 2-ethylimidazole containing solution species in the growth solution of the cadmium 2-ethylimidazolate metal–organic framework CdIF-4, and show that they are critical in the surface nucleation for the crystal growth of this material. Surface nucleation appears to be instigated by these $[Cd_x(CH_3CO_2)_y(C_5H_7N_2/C_5H_8N_2)_z]$-containing solution species and not by sole addition of the ligand molecules. The $CH_3CO_2^-$ or $Cd(CH_3CO_2)_2$ groups of the former are substituted subsequently as the framework growth proceeds. Our greater understanding of such solution species and their role in crystallization will guide future syntheses of designed functional coordination polymers.*

Understanding crystal formation is critical for the design of the rich varieties of function in which crystals are applied in modern society.[1] Numerous advances have been made in comprehending the stages of crystallization,[2] which, for solution crystallization, typically involve the formation of species in solution, nucleation, and crystal growth.[3] However, detailed nanoscale information on how these stages are connected, for example, which species identified in solution are the actual species involved in nucleation or crystal growth,[4] is often lacking especially for non-molecular crystals. There is a particular paucity of information in this regard for the crystallization of coordination polymers, an important family of compounds relevant to many fields, which includes porous metal–organic frameworks (MOFs) amongst its ranks.[5] Indeed, to the best of our knowledge, there are no reports of the identification of any metal-containing solution species that can be correlated directly with the real-time crystallization process for any coordination polymer.

To obtain such information, characterization techniques need to be used that allow for molecular identity information to be extracted from in situ crystallization experiments and the crystallization solutions involved. For MOFs, spectroscopic studies have identified various solution species involved in their formation,[6] and in situ atomic force microscopy (AFM) studies have enabled the observation of the growing of the crystal surface and provided structural information to identify surface nucleation by the ligand only.[7] We herein report a crystal growth study on the MOF CdIF-4, using a combination of in situ AFM and electrospray ionization mass spectrometry (ESI-MS). For the first time, the preassembled metal-containing solution species that are critical for surface nucleation and growth of a coordination polymer were identified.

The cadmium imidazolate framework CdIF-4 ($Cd(eIm)_2$;[8,9] HeIm = 2-ethylimidazole) is a porous MOF constructed from corner-sharing $Cd(eIm)_4$ tetrahedra in which the eIm^- ligands bridge pairs of Cd^{2+} ions to form a three-dimensional framework with the RHO topology (cubic, a = 30.887 Å, space group $Im\bar{3}m$), as shown in the Supporting Information, Figure S1. Phase-pure approximately 150 μm large rhombic dodecahedral CdIF-4 crystals (see Figures S2 and S3) were prepared that were suitable as substrate crystals for in situ AFM work. In situ crystal growth on the {110} crystal facets was observed from a room-temperature static supersaturated growth solution containing a solution used to prepare the substrate crystals that had been heated to 120 °C for 3.5 hours (see the Supporting Information for details). This *n*-butanol growth solution contained $Cd(CH_3CO_2)_2$-$(H_2O)_2$, HeIm, and growing, < 0.5 μm large CdIF-4 crystals.

In situ AFM deflection micrographs revealed crystal growth to proceed by both spiral and "birth and spread" mechanisms on the {110} facets of CdIF-4 as shown in Figures 1 and S4 (see also Movie S1). The growth islands and spirals exhibit a truncated rhombohedral morphology, which reflects the twofold symmetry of the {110} facets. Height analysis on many monolayer steps yielded a height of 2.2 ± 0.1 nm (see Figures 1 f and S4), which corresponds to the d_{110} spacing of CdIF-4.

The relatively slow rate of crystal growth during this experiment allowed for the observation of the formation of 27 two-dimensional nuclei and their growth into stable monolayer terraces. The nuclei were observed to grow into stable, 2.2 nm high monolayers through metastable sublayers; the observed heights of these sublayers encompass all the 0.1 nm incremental values in the range 0.5 nm to 2.1 nm except for 1.6 nm. For example, the nucleus shown in Figure 1 is observed to grow through metastable sublayers with heights of 0.6, 1.2, 1.5, 1.7, and 1.9 nm as shown in Figure 1 a–e. These observed sublayer step heights match well with the height differences between the solvated Cd^{2+} ions in the plane marked X in Figure 1 g and the vertical projections of all solvated Cd^{2+} ions (0.64, 0.96, 1.09, 1.41, 1.73, and 1.86 nm)

[*] R. Wagia, Dr. I. Strashnov, Prof. M. W. Anderson, Dr. M. P. Attfield
School of Chemistry, The University of Manchester
Brunswick Street, Manchester, M13 9PL (UK)
E-mail: m.attfield@manchester.ac.uk
Homepage: http://www.chemistry.manchester.ac.uk/groups/cnm/martin.htm

Supporting information and the ORCID identification numbers for the authors of this article can be found under http://dx.doi.org/10.1002/anie.201603687.

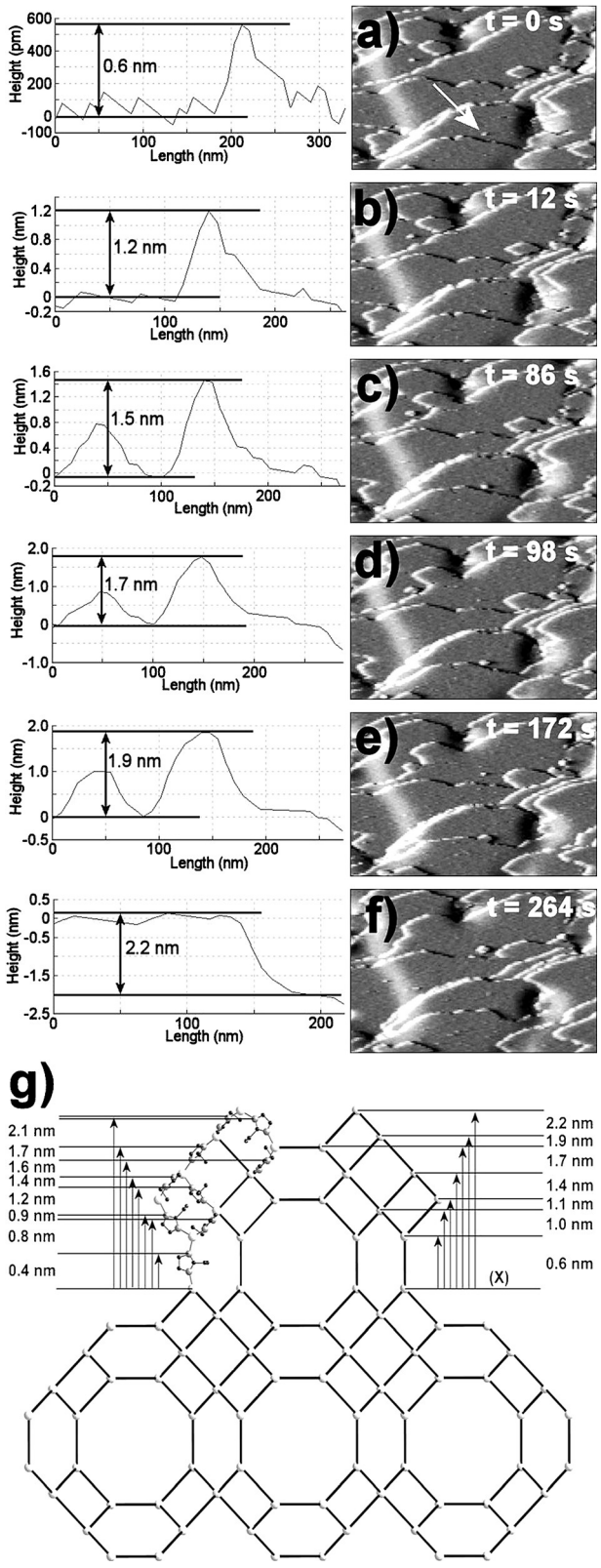

Figure 1. a–f) Real-time cross-sectional analyses and AFM deflection images of a developing growth step on a {110} face of a CdIF-4 crystal. g) The structure of CdIF-4 viewed along the <110> direction, highlighting the possible heights of the metastable sublayer steps through which the stable monolayer step is formed. The nucleus for which growth is being monitored is indicated by a white arrow in (a), and all image sizes are $1.8\times1.1\ \mu m^2$. The structure in (g) is represented in ball-and-stick mode with balls decreasing in size for Cd, N, and C. Bonds are depicted as thin gray lines, and the organic linkers as thick black lines. H atoms omitted for clarity. A color version of this Figure is provided as Figure S5.

and the uppermost nitrogen atoms of the solvated eIm^- ions (0.43, 0.84, 0.90, 1.24, 1.36, 1.57, 1.74, 2.08, and 2.09 nm) if it is assumed that the sub-step heights directly relate to the CdIF-4 crystal structure (see Figure 1 g). The lack of any metastable sublayers with heights of less than 0.5 nm, in conjunction with the other observed metastable sublayer heights, uniquely defines the surface termination of the {110} surface as consisting of solvated Q^3 Cd^{2+} ions of completed double eight ring (D8R) cages such as those marked along plane X in Figure 1 g (where Q^3 indicates that the Cd^{2+} ion is only bound into the bulk crystal structure by 3 of 4 possible linkers), and that the stable 2.2 nm monolayer steps are comprised of an inclined D8R and the edge of a single six ring (S6R) as shown in Figure 1 g. A surface termination consisting of completely closed cage structures is consistent with our findings for other MOFs.[7a,b] The observation of the growth of the surface nuclei into stable, 2.2 nm high monolayers through metastable sublayers indicates that a stable monolayer terrace grows through a process of nucleation and spreading of metastable sublayers. We have reported a similar surface crystal-growth mechanism for other MOFs.[7a,b]

The complex nature of the CdIF-4 structure and the vertical resolution of the AFM height measurements (±0.1 nm) mean that the most definitive information concerning the identity of the actual growth species and the heights of the metastable sublayers can only be ascertained for the first potential metastable sublayer heights of 0.4 nm and 0.6 nm, which correspond to the height differences between the solvated Cd^{2+} ions in the surface-termination plane X and the vertical projections to the first uppermost nitrogen atoms of solvated eIm^- ions (0.43 nm) and solvated Cd^{2+} ions (0.64 nm), respectively. The lack of any metastable sublayers with heights of less than 0.5 nm for any of the analyzed 27 two-dimensional nuclei and the observation that seven of these 27 nuclei develop through a metastable sublayer with a height of 0.6 ± 0.1 nm provide convincing evidence that successful surface nucleation is achieved only when a preassembled growth species containing a [Cd(HeIm or eIm)$_n$] unit ($n=1$ or 2) is present. This contrasts with the behavior of other MOFs, for which it has been shown that surface nucleation is achieved by addition of the organic linker only.[7] The observation that numerous nanodots appear in the in situ AFM images and then disappear in subsequent images provides additional evidence that supports this theory. The vast majority of these nanodots have heights of 0.4 ± 0.1 nm (see Figure S6), which corresponds to the uppermost nitrogen atoms of a solvated eIm^- ion (0.43 nm) binding to the Cd^{2+} ions in the surface-termination plane X. This height of 0.4 nm is also consistent with the surface addition and loss of acetate groups that are present in the growth solution, but are more likely to arise from the eIm^-

groups as they are present in excess and bind more strongly to the Cd^{2+} ions. The observation of these 0.4 nm nanodots indicates the ability of AFM to differentiate between different species in the height range of 0.4–0.6 nm within the conditions of this experiment and highlights the absence of any metastable sublayers with heights of less than 0.5 nm for any of the analyzed 27 two-dimensional nuclei that develop into 2.2 nm monolayer terraces.

Other trends observed when analyzing the heights of the growing 27 two-dimensional nuclei are that the heights for some metastable sublayers are greater than 0.6 ± 0.1 nm upon first observation, suggesting the surface addition of a preassembled $[Cd(HeIm/eIm)_n]$ ($n = 2$–4) unit. The > 0.9 nm height of some of these nuclei makes it unlikely that these nuclei develop through the initial surface addition of a preassembled [Cd(eIm)] unit followed by subsequent addition of simple $HeIm/eIm^-$ or [Cd(HeIm/eIm)] units although the temporal limitation of approximately 1–86 s between the successive imaging of the same spatial point in the experiment does not entirely preclude the possibility of smaller preassembled nucleating units being involved for these developing nuclei. Three of the 27 developing surface nuclei were also observed to have an initial height that decreases in the subsequent image before growing through successive heights into a stable extended step as shown in Figure S7. These observations imply that certain nucleating species on the surface contain fragments that exactly fit into the final CdIF-4 framework structure, for instance, a [Cd(eIm)] or $[Cd(eIm)_2]$ unit, but also contain additional units that may not form part of the final framework and are removed subsequently to enable the continued growth of the nucleus into the stable extended step.

Overall, the AFM results strongly suggest that surface nucleation of this material is only achieved when a preassembled growth species containing at least one [Cd(eIm)] unit is present, and that $HeIm/eIm^-$ groups on their own do not nucleate surface growth.

Further evidence for the likelihood of such preassembled $[Cd(HeIm/eIm)_n]$ ($n = 1$–4) units being the nucleating species was provided by ESI-MS analysis of the growth solution. Many growth species were identified in the positive- and negative-ion spectra (see Table S1 and Figures 2, S8, and S9). The more abundant Cd(HeIm/eIm)-containing growth species in the solutions are $[Cd(CH_3CO_2)(HeIm)_2]^+$, $[Cd(CH_3CO_2)(HeIm)_3]^+$, and $[Cd_2(CH_3CO_2)_3(HeIm)_2]^+$ as well as $[Cd(CH_3CO_2)_2(eIm)]^-$ in the positive-ion and negative-ion spectra, respectively, with the most abundant of these species being $[Cd(CH_3CO_2)(HeIm)_2]^+$ and $[Cd(CH_3CO_2)_2(eIm)]^-$, in the positive-ion and negative-ion spectra, respectively. We assumed that the coordination environment of the Cd^{2+} ions is completed by *n*-BuOH molecules, which may be lost during the ionization process in the mass spectrometer. The dominance of $[Cd(CH_3CO_2)(HeIm)_2]^+$ amongst the Cd(HeIm/eIm)-containing growth species agrees well with our expectation for the formation of a product of formula $Cd(eIm)_2$. The identification of a variety of species and the high abundance of the $[Cd(CH_3CO_2)(HeIm)_2]^+$ and $[Cd(CH_3CO_2)_2(eIm)]^-$ species support the results of the in situ AFM study.

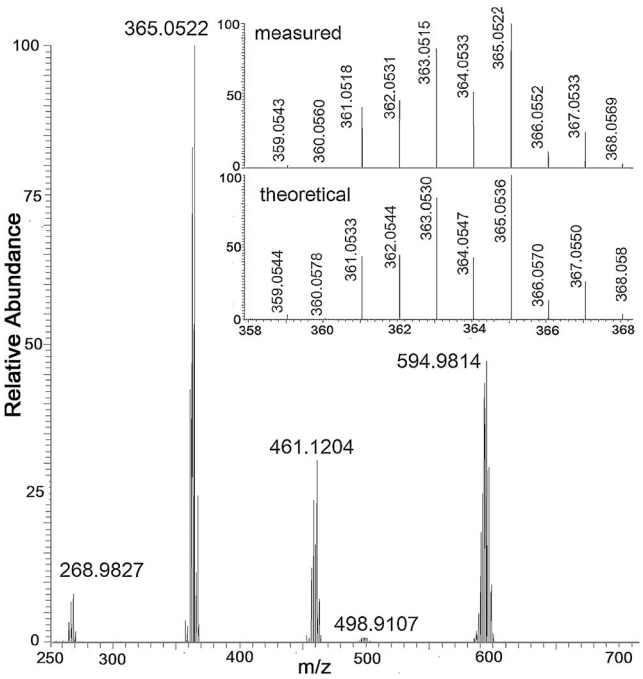

Figure 2. Positive-ion ESI-MS spectrum displaying the most abundant cadmium-containing species. The inset provides confirmation of the chemical composition for the $[Cd(CH_3CO_2)(HeIm)_2]^+$ species centered at about *m*/*z* 365 through comparison of the measured and theoretical isotopic distributions.

The observation that seven of these 27 nuclei develop through a metastable sublayer with a height of 0.6 ± 0.1 nm agrees with either deprotonated $[Cd(CH_3CO_2)(HeIm)_2]^+$ or $[Cd(CH_3CO_2)_2(eIm)]^-$ initiating nucleation (as shown for such a fragment in Figure 3a,b). The surface addition of deprotonated $[Cd(CH_3CO_2)(HeIm)_2]^+$ could also provide an initial metastable sublayer with a height of 0.8/0.9 nm depending on the orientation of the species upon addition to the surface as shown in Figure 3c,d. Moreover, addition of lower-abundance deprotonated $[Cd(CH_3CO_2)(HeIm)_3]^+$ could also generate nucleation heights of 0.8/0.9 nm as exemplified in Figure 3e–g. The latter two scenarios would explain the observation that some initial metastable sublayers have heights of > 0.7 nm, which indicates that a preassembled $[Cd(HeIm/eIm)_n]$ ($n = 2$–3) unit is the nucleating entity on the surface in these cases. The presence of $[Cd_2(CH_3CO_2)_3(HeIm)_2]^+$ as a relatively abundant species in the growth solution also provides an explanation for the observation that the developing surface nuclei initially have a height that decreases in the subsequent image before growing into a stable extended step. Addition of a > 0.6 nm large, deprotonated $[Cd_2(CH_3CO_2)_3(HeIm)_2]^+$ unit of the form shown in Figure 3h,i to the crystal surface followed by loss of the framework-incompatible $Cd(CH_3CO_2)_2$ unit would leave a remaining deprotonated $[Cd(CH_3CO_2)(HeIm)_2]^+$ unit, from which subsequent growth into the stable extended growth step could proceed. The acetate groups attached to all of these Cd(HeIm/eIm^-)-containing species are present in insufficient numbers to contradict the results of the height analysis of the AFM results and are assumed to be substituted

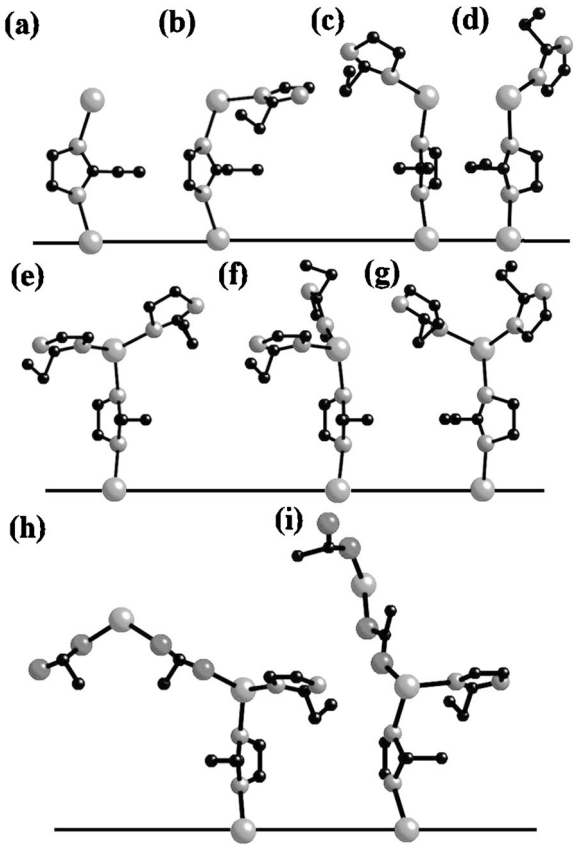

Figure 3. a–i) Representation of the initial nucleation of a new stable monolayer terrace on the crystal surface of CdIF-4 through addition of various preformed $[Cd_x(CH_3CO_2)_y(HeIm/eIm)_z]$-containing solution species of different sizes. The crystal surface is represented by Cd atoms connected by lines, and the structures of the nucleating species are derived from the crystallographic structure of CdIF-4. Atoms in order of decreasing size: Cd, O, N, C. Hydrogen atoms and terminal acetate groups that are attached to directly surface-bound Cd atoms omitted for clarity. A color version of this Figure is provided as Figure S10.

during the subsequent development of the stable extended growth step. The ESI-MS spectra also reveal the presence of eIm^-, and more noticeably H_2eIm^+, as solution species in the growth solution, making it likely that they are also involved in the growth of the stable monolayer terraces. However, the AFM results suggest that the $HeIm/eIm^-$ species do not nucleate the initial growth of the stable monolayer terraces and are more likely to be the growth species that add directly to the more poorly coordinated Q^2 and Q^1 Cd^{2+} ions that are present in the metastable sublayers as the stable monolayer terraces develop after the initial nucleation.

It is interesting to note that whereas preassembled Cd(HeIm/eIm)-containing species are critical to nucleate the surface growth of CdIF-4 in this study, only HmIm/ mIm^- (HmIm = 2-methylimidazole) was observed to be necessary to nucleate the MOF ZIF-8 in a similar study,[7a] even though the imidazole linker is in much greater excess in the former work. This may reflect the greater bond strength of a Zn–N bond compared to a Cd–N bond,[10] which will sufficiently stabilize surface HmIm/ mIm^- species to allow for further growth of the stable monolayer terrace in ZIF-8 whilst limiting the occurrence of surface nucleation for CdIF-4 via larger preassembled nucleating species that are sufficiently stable to enable further growth to a critical size instead of desorbing or dissolving.

In conclusion, in situ AFM and ESI-MS studies have revealed the crystal growth mechanism of CdIF-4 and shown that a partially preassembled component of the resulting crystal structure is the critical solution species that instigates the surface nucleation of the material. Our greater understanding of the solution species and their role in the crystal growth process will aid future syntheses and the design of coordination polymers and other extended solids as well as their crystal form and function.

Acknowledgements

This research was funded by the Ministry of Higher Education and Scientific Research, Iraq. We thank Mohammed Maqsood and Gareth Smith for collecting preliminary mass spectra.

Keywords: atomic force microscopy · coordination polymers · crystal growth · metal–organic frameworks · nucleation

How to cite: *Angew. Chem. Int. Ed.* **2016**, *55*, 9075–9079
Angew. Chem. **2016**, *128*, 9221–9225

[1] a) B. Seoane, S. Castellanos, A. Dikhtiarenko, F. Kapteijn, J. Gascon, *Coord. Chem. Rev.* **2016**, *307*, 147–187; b) O. Shekhah, J. Liu, R. A. Fischer, C. Wöll, *Chem. Soc. Rev.* **2011**, *40*, 1081–1106; c) C. Park, J. E. Park, H. C. Choi, *Acc. Chem. Res.* **2014**, *47*, 2353–2364; d) N. Blagden, M. de Matas, P. T. Gavan, P. York, *Adv. Drug Delivery Rev.* **2007**, *59*, 617–630; e) J. D. Rimer, M. Kumar, R. Li, A. I. Lupulescu, M. D. Oleksiak, *Catal. Sci. Technol.* **2014**, *4*, 3762–3771; f) G. Reiter, *Chem. Soc. Rev.* **2014**, *43*, 2055–2065.

[2] a) P. Cubillas, M. W. Anderson in *Zeolites and Catalysis* (Eds.: J. Cejka, A. Corma, S. Zones), Wiley-VCH, Weinheim, **2010**, pp. 1–55; b) M. P. Attfield, P. Cubillas, *Dalton Trans.* **2012**, *41*, 3869–3878; c) G. Férey, M. Haouas, T. Loiseau, F. Taulelle, *Chem. Mater.* **2014**, *26*, 299–309; d) J. J. De Yoreo et al., *Science* **2015**, *349*, aaa6760; e) M. H. Nielsen, S. Aloni, J. J. De Yoreo, *Science* **2014**, *345*, 1158–1162.

[3] a) J. W. Mullin in *Crystallization*, Butterworth Heinemann, Oxford, **2001**, pp. 1–477; b) I. Sunagawa in *Crystals*: *Growth*, *Morphology and Perfection*, Cambridge University Press, Cambridge, **2005**, pp. 1–278.

[4] D. Gidalevitz, R. Feidenhans, S. Matlis, D. M. Smilgies, M. J. Christensen, L. Leiserowitz, *Angew. Chem. Int. Ed. Engl.* **1997**, *36*, 955–959; *Angew. Chem.* **1997**, *109*, 991–995.

[5] J. R. Long, O. M. Yaghi, *Chem. Soc. Rev.* **2009**, *38*, 1213–1504.

[6] a) S. Surblé, F. Millange, C. Serre, G. Férey, R. I. Walton, *Chem. Commun.* **2006**, 1518–1520; b) J. A. Rood, W. C. Boggess, B. C. Noll, K. W. Henderson, *J. Am. Chem. Soc.* **2007**, *129*, 13675–13682; c) I. H. Lim, W. Schrader, F. Schüth, *Chem. Mater.* **2015**, *27*, 3088–3095; d) G. Seeber, G. J. T. Cooper, G. N. Newton, M. H. Rosnes, D. L. Long, B. M. Kariuki, P. Kogerler, L. Cronin, *Chem. Sci.* **2010**, *1*, 62–67; e) T. D. Petersen, G. Balakrishnan, C. L. Weeks, *Dalton Trans.* **2015**, *44*, 12824–12831; f) M. Haouas, C. Volkringer, T. Loiseau, G. Férey, F. Taulelle, *Chem. Mater.* **2012**, *24*, 2462–2471.

[7] a) P. Y. Moh, P. Cubillas, M. W. Anderson, M. P. Attfield, *J. Am. Chem. Soc.* **2011**, *133*, 13304 – 13307; b) P. Cubillas, M. W. Anderson, M. P. Attfield, *Chem. Eur. J.* **2012**, *18*, 15406 – 15415; c) P. Cubillas, K. Etherington, M. W. Anderson, M. P. Attfield, *CrystEngComm* **2014**, *16*, 9834 – 9841.
[8] Y. Q. Tian, S. Y. Yao, D. Gu, K. H. Cui, D. W. Guo, G. Zhang, Z. X. Chen, D. Y. Zhao, *Chem. Eur. J.* **2010**, *16*, 1137 – 1141.
[9] O. Karagiaridi, W. Bury, A. A. Sarjeant, C. L. Stern, O. K. Farha, J. T. Hupp, *Chem. Sci.* **2012**, *3*, 3256 – 3260.
[10] I. E. Gümrükcüoglü, J. Jeffery, M. F. Lappert, J. B. Pedley, A. K. Rai, *J. Organomet. Chem.* **1988**, *341*, 53 – 62.

Received: April 15, 2016
Published online: June 8, 2016

